

RESOLUTION OF BIOLOGICAL MICROSTRUCTURE THROUGH *IN SITU* FLUORESCENCE EMISSION SPECTRA

AN OCEANOGRAPHIC APPLICATION USING OPTICAL FIBERS

By Timothy J. Cowles and Russell A. Desiderio

ONE OF THE CHALLENGES we face as oceanographers is the wide range of spatial and temporal scales over which we must measure the physical, biological, and chemical properties and processes in the ocean. The constraints of available technologies have required discrete sample collection with bottles or nets to define the distribution of bulk biological and chemical properties and processes. These sampling constraints have confined us to a relatively coarse-scale resolution of the biological and chemical characteristics of the upper ocean. In contrast, physical oceanographic instrumentation has provided definition of temperature, salinity, and density over a much wider range of spatial scales, from centimeters (microscale) to thousands of kilometers (basin scale). This mismatch in sampling resolution between physical and biological/chemical properties is particularly critical at the microscale, where it is likely that biological and chemical distributions and processes are constrained by finescale and microscale physical processes. It is, therefore, critical to our understanding of the linkages between small-scale physics, biology, and chemistry that we address this mismatch in sampling scales through new approaches to instrumentation to measure biological microstructure.

The need for sub-1-m resolution of plankton distributions has long been recognized (e.g., Cassie, 1963), and this need has become increasingly important as laboratory and field experiments have documented the complex interrelationships of microbes and protists in plankton ecology. Additional laboratory evidence has documented the complex behavioral responses of mesozooplankton to various chemical and me-

chanical stimuli. Other studies of small-scale patchiness of plankton abundance have revealed considerable variability over vertical distances of tens of centimeters.

These laboratory and field observations led us to investigate the coupling between the small-scale physical environment and the small-scale distribution of phytoplankton. Only with coincident biological and physical measurements over the same spatial scales could we begin to relate the biological patterns of distribution that were important to zooplankton to the physical processes occurring over small vertical scales. Our objective was to measure a representative biological signal over the same vertical scales (i.e., centimeters) as temperature, conductivity, and microscale velocity shear could be measured by the sensors on a microstructure profiler (Caldwell *et al.*, 1985). We chose phytoplankton pigment fluorescence as the representative biological signal, because it can be measured easily *in situ* and it provides a rough index of phytoplankton biomass. The practical problem we faced was how to obtain sufficient fluorescence signal at centimeter spatial scales from a free-falling profiler that could accommodate only a penlight-sized fluorescence sensor.

During the 1980s, Dr. Tomas Hirschfeld and his group at the Lawrence Livermore National Laboratory were developing optical techniques for the remote detection of chemical signals. These analytical chemists were transmitting monochromatic excitation along an optical fiber, the distal end of which was modified to create an optical sensor (optrode). In the typical application, the substance to be measured would undergo a chemical reaction with a substrate in the optrode, and the resultant product would fluoresce. A portion of the fluorescence signal would travel back up the optical fiber towards the source and would be split off to a detector. Discussions with Dr. Hirschfeld just before

. . . physical
oceanographic
instrumentation has
provided definition of
temperature, salinity,
and density over a
much wider range of
spacial scales, . . .

T.J. Cowles and R.A. Desiderio, College of Oceanic and Atmospheric Sciences, Oregon State University, Corvallis, OR 97331, USA.

his untimely death in 1986 led to our active collaboration with his associate, Dr. S. Michael Angel, and ultimately resulted in the adaptation of this optical fiber application to biological oceanography (Cowles *et al.*, 1989, 1990, 1993; Myrick *et al.*, 1990; Angel *et al.*, 1991; Desiderio *et al.*, 1993).

We describe in this paper several aspects of the technical adaptation and modification of a fiber optical application into oceanography. We present some of the details that we had to consider during the design and fabrication stages of our instrument development and discuss some of the problems encountered during the different stage of prototype development. Additional specific details about the instrumentation can be found in Desiderio *et al.* (1993), while examples of small-scale biological structure can be found in Cowles *et al.* (1993).

Technical Approach

We coupled a laser/fiber optic fluorometer system to a free-fall microstructure profiler (Fig. 1), as described in Cowles *et al.* (1990) and Desiderio *et al.* (1993). A shipboard Argon laser was used to generate either 488- or 514-nm light, which was launched into 200 m of 200- μm core optical fiber.

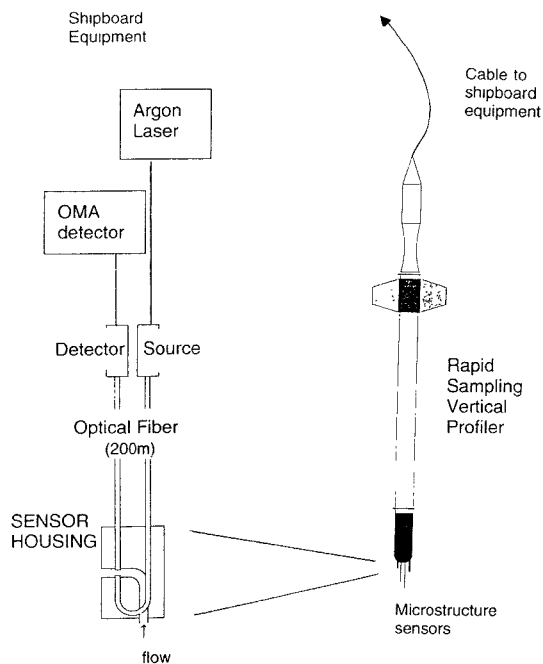


Fig. 1: Schematic diagram of the Rapid Sampling Vertical Profiler (RSVP) with sensors in the nosecone for temperature, horizontal velocity shear, and fluorescence. The SENSOR HOUSING on the left represents the small probe for collection of fluorescence, with internal optical fibers as described in the text. The 200-m optical fibers connected the fluorescence probe to the shipboard laser source and optical multichannel array (OMA) detector, both mounted on a vibration-isolated optical bench. See text for additional details.

This excitation fiber was connected to a custom sensor (Angel *et al.*, 1991), which contained a flow-through port for water (and phytoplankton) to pass through the illuminated sample volume. The resulting pigment fluorescence was collected by a 200-m length of 400- μm core optical fiber and was delivered to an intensified optical multichannel diode array detector on the ship. We collected fluorescence emission spectra (540–760 nm) at 30 Hz, providing approximately 2 cm vertical resolution at an instrument drop rate of 50 cm/s. Coincident measurements of microscale temperature and horizontal velocity shear provided the physical context in which to interpret the spatially highly resolved fluorescence emission data.

The successful development of our application depended upon the characteristics of the full optical path, which included our optical fibers, our fluorescence sensing probe, and the optical connectors. Optical fibers have been used for digital transmission of preprocessed data at near-IR wavelengths in various oceanographic applications, but our application required the transmission of an analog visible optical signal from a sample volume to a shipboard detector. The successful use of optical fibers in our application therefore depended upon the transmission characteristics of the fibers within the wavelength range of fluorescence emission by the photosynthetic pigments of the phytoplankton, as well as at the excitation wavelengths.

Technical Considerations of Optical Fibers as Analog “Light Pipes”

We evaluated several multimode optical fibers (Table 1) for use as optical cables (Table 2) and as short optical conduits within the custom fluorescence probe (Table 3). We used multimode optical fibers rather than single mode fibers because we could more easily launch our excitation light into a multimode fiber and maintain good optical alignment under shipboard conditions. (Multimode fibers have a large core radius relative to wavelength. Single-mode optical fibers, on the other hand, have a relatively small core radius and support only one guided mode. The resultant high bandwidth and low attenuation make them the preferred fiber for longer distance digital communication.) Before deployment, each 200-m section of optical fiber was provided with a braided Kevlar sleeve for strain relief and then covered with an outer cabling. The optical fiber is placed under tension during the cabling process and may undergo some stress, which alters the transmission characteristics beyond the manufacturer’s specifications. It is therefore important to verify independently the transmission properties of each cabled fiber.

Spectral Attenuation and Background Emission

Optical fibers have been designed to be effective links in the communications industry due to their

... successful development of our application depended upon the characteristics of the full optimal path, ... our fluorescence sensing probe, and the optical connectors.

Table 1
Characteristics of optical fibers used in the microstructure profiling application

Fiber	Type	Company	Core	Cladding	Buffer	NA
200 μm DIA	ST200D-SY, Diaguide	Mitsubishi Cable	200 μm silica	250 μm silica	1.0 mm black nylon	0.2
400 μm DIA	ST400E-SY, Diaguide	Mitsubishi Cable	400 μm silica	500 μm silica	1.3 mm black nylon	0.2
200 μm HCR	HCR-M0200T-05	Ensign Bickford	200 μm silica	230 μm silica	0.50 mm clear tefzel	0.3
400 μm HCR	HCR-M0400T-06	Ensign Bickford	400 μm silica	430 μm silica	0.73 mm clear tefzel	0.3

NA, numerical aperture.

wide bandwidth (single mode fibers) and efficient transmission at specific wavelengths in the near-IR. Optical fibers become much less transmissive as the wavelength moves to shorter wavelengths, with many optical fibers having a 30–40 dB per kilometer attenuation at a transmission wavelength of 500 nm compared with 6–10 dB per kilometer at 700 nm. As mentioned above, the stress placed on the optical fiber during the cabling process can increase attenuation at all wavelengths. These attenuation factors place constraints on the length of optical fibers that can be used to deliver specific excitation wavelengths to distant locations. In our application, we needed to deliver between 5 and 10 mW of 488 or 514 nm light into the sample volume of our fluorescence sensor. To overcome the attenuation in propagating through 200 m of fiber, as well as the smaller losses due to propagation through interference filters and optical connectors, we estimated that we needed to launch ~50–100 mW of each of the major Argon lines to illuminate the sample volume at the distal end of the fiber.

A portion of the excitation light that is inelastically scattered within the fiber is detectable as background fiber emission (Dakin and King, 1983; Myrick *et al.*, 1990; Desiderio *et al.*, 1993). This background fiber emission often overlaps with the signal of interest, as illustrated in Figure 2. In a single-fiber application for photosynthetic pigment

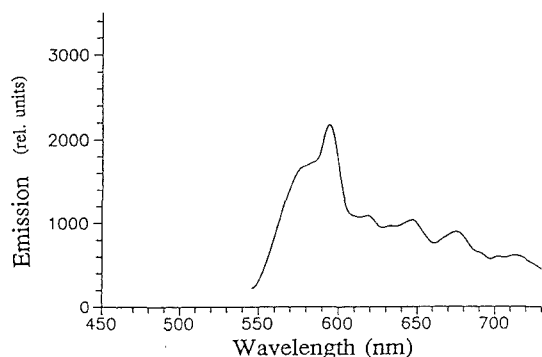


Fig. 2: Background emission spectrum from 100 m of silica-clad fiber (distal end in air). A 570-nm long-pass filter was used to discriminate against short wavelength fiber emission. Spectrum has been smoothed using a Fourier transform algorithm with a 7-nm window.

fluorescence, the combined effects of background emission from the optical fiber and of excitation light attenuation will limit fiber length to <100 m for the highest quality silica-clad fibers (Desiderio *et al.*, 1993). These constraints may be acceptable in applications that do not require long lengths of fiber. Additional discussion of the limitations of single-fiber applications for fluorescent detection of phytoplankton pigment can be found in Desiderio *et al.* (1993).

Background fiber emission can also present problems in a dual-fiber configuration. The light emerging from the excitation fiber consists of the monochromatic light from the laser, plus all the broadband fiber emission generated within the fiber (e.g., Fig. 2). Well-designed interference filters are therefore required to block all the unwanted wavelengths from reaching the sample volume, especially those at the fluorescence signal wavelength. In addition, interference filters that block all of the excitation wavelengths are required in front of the detection fiber, thus minimizing the generation of background fiber emission within the detection fiber.

Internal Standards for Signal Correction

It has been demonstrated that light transmission through optical fibers is attenuated as a result of fiber bending (Myrick *et al.*, 1990). We used the Raman scattering of water as an internal standard to correct for possible transmission losses due to bending of the cabled fibers during deployment. In most profiles, however, we did not detect substantial attenuation because of bending of the main excitation and emission fibers, and the Raman correction was rarely >10%.

We did detect, however, a significant difference in the temperature response of the individual fluorescence sensors (Table 3). These sensors contained a 200- μm core excitation fiber that had to bend through a 4-mm radius of curvature, and a 400- μm core collection fiber that did not bend within the sensor. The sensor probe constructed with plastic-clad fiber [numerical aperture (NA) = 0.3] as the excitation fiber (probe #3) had a consistent, relatively constant water Raman scattering response through each profile (Fig. 3). In contrast, the silica-clad excitation fibers (NA = 0.2) in probes #1, #2, and #5 had a definite response to water temperature (Fig. 4). Note the distinct

Well-designed interference filters are . . . required to block all the unwanted wavelengths from reaching the sample volume.

Table 2
Composition of optical fiber cables

Cable Pair	Excitation Cable	Emission Cable
DA	200 μm core DIA fiber; standard MC cable; braided Kevlar sleeve, black vinyl jacket (opaque to sunlight)	400 μm core HCR fiber; "Avioptics" EB cable; braided Kevlar sleeve, lavender fluoropolymer jacket (permeable to sunlight)
CC	200 μm core HCR fiber; "C-series" EB cable; braided Kevlar sleeve, orange polyurethane jacket (permeable to sunlight)	400 μm core HCR fiber; "C-series" EB cable; braided Kevlar sleeve, orange polyurethane jacket (permeable to sunlight)
AH	200 μm core HCR fiber; "Avioptics" EB cable; braided Kevlar sleeve, lavender fluoropolymer jacket (permeable to sunlight)	400 μm core HCR fiber; custom EB cable; braided Kevlar sleeve, blue-green hytel jacket (opaque to sunlight)

change in the water Raman signal as the probe moved through the thermocline into cooler water. We also tested these probes by immersing them in a temperature-regulated water bath in the laboratory and found the same temperature response as shown in Figure 4. Moreover, the temperature response was reversible. We suspect that the thermal contraction of the metal housing of the probe in cooler water increased the stress on the silica-clad excitation fiber along the sharp radius of curvature at the tip of the probe. The additional stress on the bent fiber caused an increase in attenuation of the excitation light, thereby reducing the amplitude of the water Raman scattering signal.

These results have important implications for the detection of luminescent/fluorescent signals via optical fibers. It is crucial that the detection scheme used for the species of interest, whether it be photosynthetic pigments or dissolved organic compounds, has an internal standard at some wavelength outside the emission band of the species of interest. Such an internal standard allows for the detection and correction for signal attenuation due to fiber transmission losses from bending, temperature, and possibly pressure effects. These attenuation effects become more important for applications requiring environmental exposure of long lengths of optical fiber.

Other Technical Issues

Penetration of Sunlight and Bright Deck Light into Optical Fibers

We found that the outer cabling on some of the fibers listed in Table 2 allowed sunlight and bright deck light to penetrate into the cladding/core of the fiber, creating a broadband, background signal in the fiber that altered the limits of fluorescence detection. The black vinyl cable on the Diaguide fiber was opaque to sunlight, as was the hytel cable on the Ensign Bickford fiber (Table 2).

Optical Connections

It is inevitable that optical fibers in cables that connect a remote instrument to the vessel will break during routine instrument deployments. It may also be desirable to change sensor probes during a deployment sequence. It is therefore necessary to have optical connectors between the fiber and the sensor located at the distal end of the fiber/cable assembly. These connections must be watertight because seawater intrusion can change the transmissivity of the optical fiber. We used SMA 906 fiber-optic connectors to couple the cabled fibers to our custom sensor probe and sealed the outside of the SMA connectors with electrical insulation putty and electrical tape. We did not ob-

Table 3
Characteristics of fluorescence probes

Probe	Excitation Fiber:		Emission Fiber:		Filter Set	Temperature Dependence of Fluorescence Signal?	Flashlight Test 1*	Flashlight Test 2†
	Core Size, μM	Type	Core Size, μM	Type				
1	200	DIA	400	DIA	Thick	Yes	None	Orange
2	200	DIA	400	HCR	Thick	Yes	None	Orange
3	200	HCR	400	HCR	Thick	No	Blue-green	Orange
4	200	DIA	400	DIA	Thin	—	None	Orange
5	200	DIA	400	HCR	Thin	Yes	Blue-green	Orange

* Color of white light transmitted through excitation path.

† Color of white light transmitted through emission path.

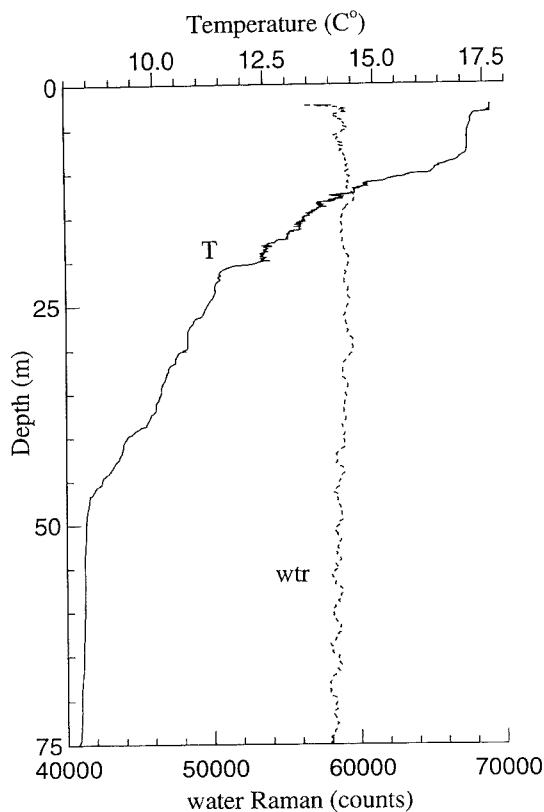


Fig. 3: Vertical profile of temperature at a station ~200 km off the Oregon coast, with the associated profile of water Raman scattering as detected with probe #3 (Table 3) with 488-nm excitation from an Argon ion laser.

serve water intrusion with this connection method, but we did find that extreme care was required to ensure a consistent, reproducible optical connection between the cabled fiber and the sensor probe. The SMA connectors provide a mechanical fiber face: fiber face connection. We found that SMA 906 connectors provided more mechanical stability than SMA 905 connectors, which lack an alignment collar around the fiber tips within the connector. If the fiber faces are not well aligned, then an unknown amount of signal may be lost. If the connection is not tight, then the transmitted signal will vary as a function of mechanical stress. Careful diagnostic tests of each optical connection are therefore essential in these applications.

Optical fibers and winches

We found that a dual-fiber system (two-cabled optical fibers connected to a dual-fiber sensor probe) provided sufficient signal to resolve pigment fluorescence over vertical scales of 5 mm to 2 cm (depending on drop speed) from a free-fall microstructure profiler. We have successfully deployed this prototype under a range of wind and sea-state conditions, from calm seas to rough conditions with winds >12 m/s. Repeated profiles were obtained by dropping the profiler with slack

cables to achieve free-fall and unperturbed microscale velocity shear measurements and then retrieving the profiler by hand at the end of each drop. We obtained several short time series (1–2 hr duration) with this deployment technique, but longer time series were not possible in the absence of a winching method for the double-optical fiber system. A reliable winching system requires optical slip rings that have known and consistent transmission characteristics throughout the angular rotation of the optical connection. We did not find an affordable and satisfactory winch arrangement for a dual optical fiber system that could preserve the signal amplitude through the full angular rotation of the optical slip rings. This is a solvable problem for digital systems, which require only that signal amplitudes exceed threshold values of detection.

Summary of Specific Technical Issues for Optical Fiber Use in Oceanography

Our experience suggests that long lengths of optical fiber can be used successfully to transmit

A reliable winching system requires optimal slip rings . . .

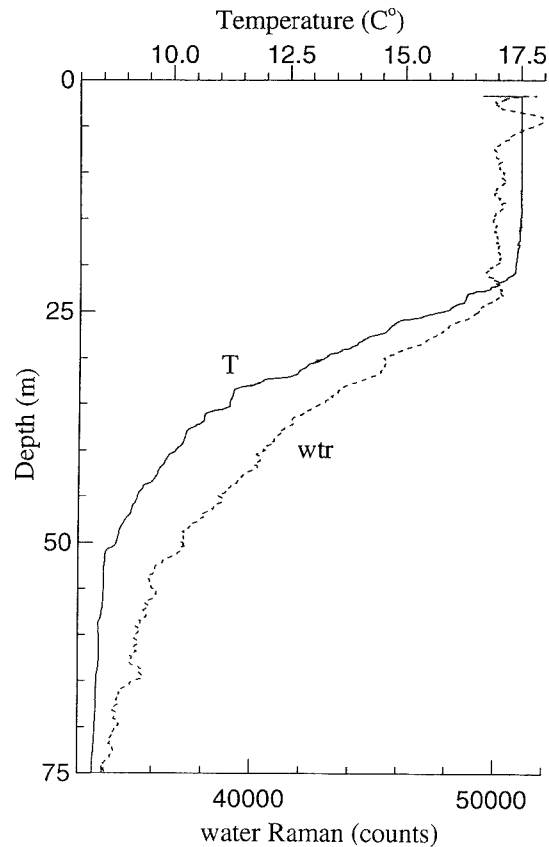


Fig. 4: As in Figure 3, but with probe #5 (Table 3), which had silica-clad fiber in the excitation portion of the fluorescence sensor. Note the distinct temperature response of this probe, particularly in comparison to the response of probe #3 (Fig. 3), which used plastic-clad fiber as the excitation fiber.

“analog” optical data from remote instruments, provided that care is taken to preserve the amplitude of the signal throughout the optical path. We emphasize the following problem areas:

- reduced sensitivity due to internal luminescence within a fiber;
- need for an internal standard to characterize signal attenuation due to fiber stress mechanisms;
- consistent, reproducible optical connections under water;
- optical slip rings on winches; and
- temperature effects on the transmission of specific fibers as a function of bending radius.

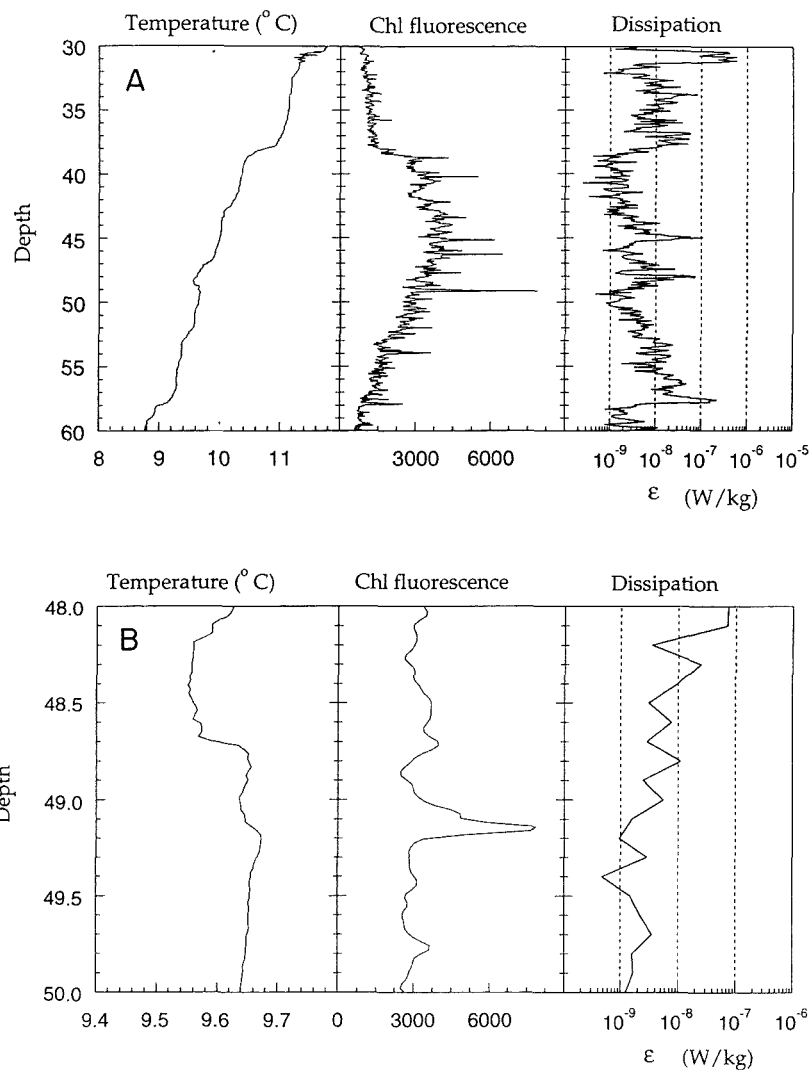


Fig. 5: Vertical profile of temperature, chlorophyll fluorescence, and turbulent kinetic energy dissipation at a station ~200 km off the Oregon coast. (A) The depth range between 30 and 60 m shows the characteristic distribution of a few thin layers of enhanced chlorophyll fluorescence. Note the presence of thin layers near local minima in dissipation. (B) An expanded view of the 48- to 50-m segment of the profile, showing the 20-cm thick layer, which has 2.5 times the local (± 1 m) fluorescence.

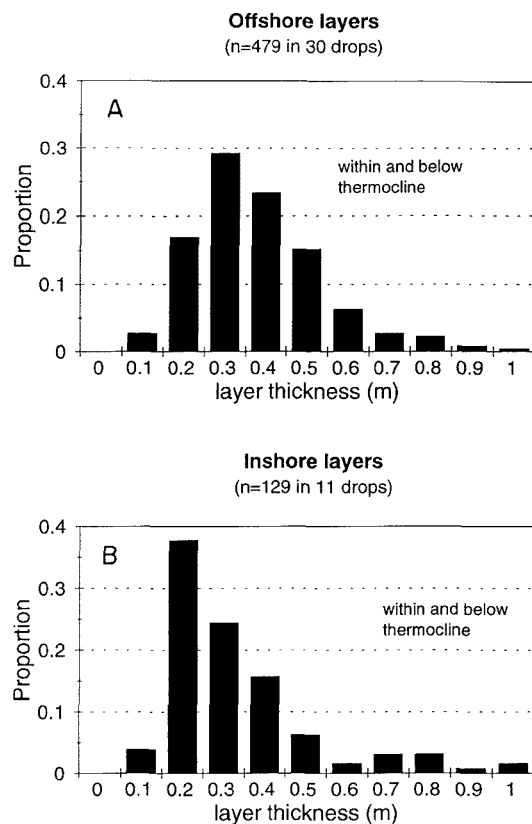


Fig. 6: Frequency distribution of the thickness of thin layers of chlorophyll fluorescence within and below the thermocline (A) in offshore waters, and (B) at the shelf break off the Oregon coast. We found that the size distribution of thin layers at the offshore station did not vary between successive nights of observations. Note that the mode of the distribution from both offshore and shelf break stations is between 0.20 and 0.40 m.

Application of Fiber Optic System to resolve Biological Microstructure

We have successfully used the laser/fiber optic fluorometer/profiler to obtain time series of microstructure temperature, fluorescence, and microscale horizontal velocity shear. Many of the profiles have revealed persistent small-scale structure in phytoplankton biomass within the euphotic zone at oceanic and shelf-break locations. We have found two- to threefold increases in pigment fluorescence over vertical scales of 10–40 cm (Fig. 5) and have found that most of the thin layers of fluorescence fall within this size range of thickness (Fig. 6). In many profiles, thin layers of fluorescence are associated with local minima in turbulent kinetic energy dissipation (Fig. 5). Persistence of these small-scale features has important consequences for planktonic processes.

Resolution of emission spectra via optical fibers also has enabled us to detect spectral shifts in fluorescence emission as a function of depth

without discrete sample collection. We found that the peak emission of phycoerythrin fluorescence shifted to longer wavelengths (Cowles *et al.*, 1993) as the profiler dropped through the euphotic zone, suggesting a compositional change in the assemblage of autotrophic organisms containing phycobilin pigments. This compositional change was confirmed by microscopic enumeration of microplankton from separately collected discrete water samples (see Cowles *et al.*, 1993, for details). These results suggest that *in situ*, nontaxonomic characterization (Yentsch and Phinney, 1985) of autotrophic plankton could be a realizable research objective.

In summary, we have adapted fiber optic techniques to observe small-scale biological structure at measurement scales that are coincident with physical measurements. We expect that the ongoing development of bio-optical instrumentation of this type will lead to a better understanding of the linkages between physical/biological/chemical processes at small scales.

Acknowledgements

This work has been supported by the National Science Foundation and the Office of Naval Research. These measurements could not have been made without the assistance of Dr. James Moum, who collaborated on the integration of the fluorescence sensor with the Rapid Sampling Vertical Profiler (RSVP) and its microscale measurements of physical properties. We are grateful to Drs. S. Michael Angel and Michael Myrick for their technical expertise in the development of the fiber optic probe, to Mr. Darrel Garvis for fabrication of probes, and to Dr. Mary-Elena Carr for her assistance in data analysis and interpretation.

References

- Angel, S.M., T.J. Kulp, M.L. Myrick, K.C. Langry, 1991: Development and applications of fiber-optic sensors. In: *Chemical Sensor Technology*, vol. 3, N. Yamazoe, ed., Kodansha Ltd, and Elsevier Science Publishers, BV, 163–183.
- Caldwell, D.R., T.M. Dillon, and J.N. Moum, 1985: The rapid sampling vertical profiler: an evaluation. *J. Atmos. Oceanic Tech.*, 3, 615–625.
- Cassie, R.M., 1963: Microdistribution of plankton. *Oceanogr. Mar. Biol. Ann. Rev.*, 1, 223–252.
- Cowles, T.J., R.A. Desiderio, J.N. Moum, M.L. Myrick, D. Garvis, and S.M. Angel, 1990: Fluorescence microstructure using a laser/fiber optic profiler. *Ocean Optics X, Proc. SPIE*, 1302, 336–345.
- Cowles, T.J., R.A. Desiderio, and S. Neuer, 1993: In situ characterization of phytoplankton from vertical profiles of fluorescence emission spectra. *Mar. Biol.*, 115, 221–227.
- Cowles, T.J., J.N. Moum, R.A. Desiderio, and S.M. Angel, 1989: In situ monitoring of ocean chlorophyll via laser-induced fluorescence backscatter through an optical fiber. *Appl. Opt.*, 28, 595–600.
- Dakin, J. and A. King, 1983: Limitations of a single optical fiber fluorimeter system due to background fluorescence. In: *Proceedings, First International Conference on Optical Fiber Sensors*. Optical Society of America, Washington DC, 195–199.
- Denman, K.L. and T.M. Powell, 1984: Effects of physical processes on planktonic ecosystems in the coastal ocean. *Oceanogr. Mar. Biol. Annu. Rev.*, 22, 125–168.
- Desiderio, R.A., T. J. Cowles, J.N. Moum, and M.L. Myrick, 1993: Microstructure profiles of laser-induced chlorophyll fluorescence spectra: evaluation of backscatter and forward-scatter fiber-optic sensors. *J. Atmos. Oceanic Tech.*, 10, 209–224.
- Myrick, M.L., S.M. Angel, and R.A. Desiderio, 1990: Comparison of some fiber optic configurations for measurement of luminescence and Raman scattering. *Appl. Opt.*, 29, 1333–1344.
- Yentsch, C.S. and D.A. Phinney, 1985: Spectral fluorescence: an ataxonomic tool for studying the structure of phytoplankton populations. *J. Plank. Res.*, 7, 617–632. □